J|A|C|S
COMMUNICATIONS

Published on Web 04/27/2006

Negative Differential Resistance and Hysteresis through an Organometallic Molecule from Molecular-Level Crossing

Rui Liu,[†] San-Huang Ke,[†,‡] Harold U. Baranger,*[,‡] and Weitao Yang*[,†]

Departments of Chemistry and Physics, Duke University, Durham, North Carolina 27708-0305

Received October 17, 2005; E-mail: baranger@phy.duke.edu; weitao.yang@duke.edu

Electrical conduction through molecules is a basic chemical property which has been investigated intensively in recent years.[1] Well-developed organic synthesis enables exploration of a large space of molecular electronic structures with a wide variety of transport properties. Through redox, charging, and conformational flexibility, molecules can, for instance, switch current,[2] exhibit negative differential resistance (NDR),[3] and even show hysteresis[4] under applied bias.

To look for additional mechanisms of NDR, it is fruitful to consider analogies with semiconductor structures. In a quantum double-dot system,[5] electron tunneling is resonantly enhanced when two discrete levels, one in each dot, become aligned. Upon increase of the applied bias, the two levels fall out of alignment and the current drops, thus causing NDR. Following this, we look into diblock structured molecules — a molecular double dot (MDD). To realize a MDD, the molecule should bear spatially separated functional groups with localized and discrete molecular levels. In addition, the voltage should drop between the two groups, an essential requirement leading to the crossing of the localized levels as bias is scanned. Molecules containing metallocene moieties[6] appear to be a good choice. The frontier orbitals of a metallocene largely preserve the d character of the transition metal; the cyclopentadienyl (CP) ligands spatially and energetically confine the d states, making the transition metal atom an intrinsic molecular dot. Additionally, as those d states are higher in energy than π-bonding orbitals of common organic conjugated systems, low-bias operation can be realized. In fact, conduction through single organometallic molecules has been measured in a number of cases recently.[7]

Our implementation[8] of the DFT−Green function approach[9] is used for the electronic transport calculations. We use double-ζ plus polarization basis sets (DZP)[10] and optimized Troullier−Martins pseudopotentials. The PBE version of the generalized gradient approximation (GGA) functional[11] is adopted for exchange-correlation, and the SIESTA package[10] is used for the unrestricted DFT calculation.

We show here in Figure 1 that an organometallic MDD junction does show NDR; in addition, a hysteretic jump at ∼1.2 V is present. When the voltage is swept forward from zero (i.e., the self-consistent Hamiltonian matrix at lower bias is used as initial input for larger bias), the current initially remains less than 0.1 μA and then increases to 2.9 μA in less than 0.4 V. Upon approaching 1.2 V, the current drops abruptly to 0.1 μA and stays low at higher bias, resulting in a large NDR peak with a peak-to-valley ratio of 30:1. When the voltage is swept backward (i.e., using a higher bias result as input) from a voltage higher than 1.2 V, the $I-V$ curve is completely different from that of the forward scan.

To understand why the sharp increase in current starts at 0.8 V, we study in Figure 2 the evolution of molecular levels as a function of bias voltage. First, according to the density of states projected on the Co and Fe atoms (panel a), we identify molecular orbitals

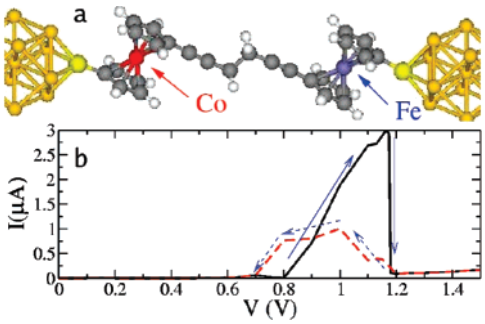

Figure 1. (a) Molecular double dot (MDD) sandwiched between rodlike gold electrodes. Gold, white, gray, red, blue, and yellow denote gold, hydrogen, carbon, cobalt, iron, and sulfur atoms, respectively. The molecule contains a cobaltocene moiety on the left and ferrocene on the right. The highest occupied molecular orbital (HOMO) of ferrocene is the nonbonding orbital a_{1g}, and e^*_{1g} is the lowest unoccupied molecular orbital (LUMO). Isolated cobaltocene has one unpaired electron; its e^*_{1g} antibonding orbital is half-occupied.[6] An insulating barrier is generated by the C_2H_4 unit, which is linked to those molecular dots by triple bonds. The molecule is adsorbed at four-fold hollow sites of (001) semi-infinite 4 Å × 4 Å rodlike gold leads. (b) $I-V$ characteristic of the molecule in panel a. Positive voltage is applied on the left lead. The black curve, scanned from 0 to 1.5 V, shows a sharp peak and dramatic NDR. The dashed red curve shows the current when scanned from voltage higher than 1.2 V to 0 V.

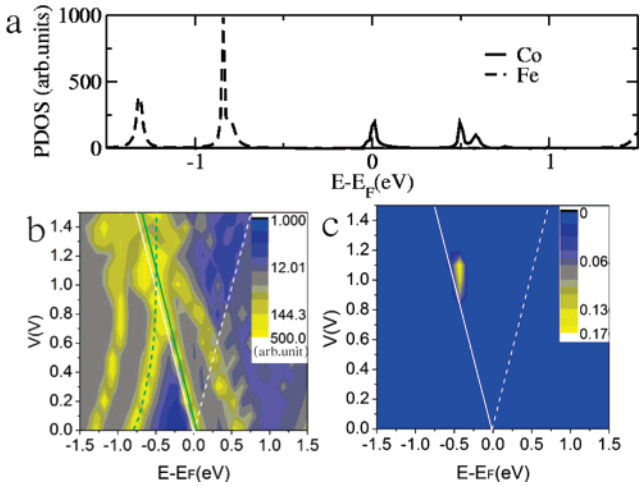

Figure 2. (a) Projected density of states (PDOS) on the iron (dashed) and cobalt (solid) atoms. (b) Evolution of PDOS on the molecule and (c) transmission probability as functions of electron energy and bias voltage. The triangle defined by white lines is the bias window; solid and dashed lines refer to the chemical potentials of the left and right leads, respectively. Solid and dashed green lines mark the PDOS localized on cobaltocene and ferrocene, respectively. Note that the sharp peak of the ferrocene HOMO in panel a is truncated from 1000 to 500 in magnitude in panel b to make other states more visible. The transmission sharply increases when the cobaltocene and ferrocene levels cross.

[†] Department of Chemistry.
[‡] Department of Physics.

10.1021/ja057054z CCC: $33.50

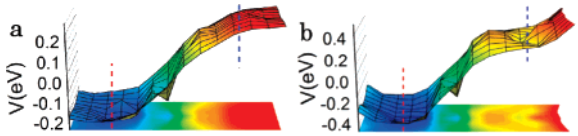

Figure 3. Potential drop through the molecule at an applied bias of (a) 0.5 V and (b) 1 V. Dashed red and blue lines indicate where the Co and Fe atoms are located, respectively. At low bias, the voltage drops across the alkane barrier, while in the resonant regime there is significant drop between the leads and the metallocene moieties.

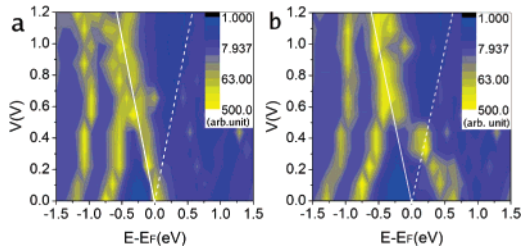

Figure 4. PDOS evolution when swept from high to low bias. (a) Spin-up and (b) spin-down components.

localized at ferrocene and cobaltocene. Panel b then shows how these orbitals move as voltage is applied.

At low bias, despite the cobaltocene state within the bias window (indicated by solid green line), incident electrons encounter a large barrier consisting of the central and right parts of the system, yielding low transmission (Figure 2c). Note that the ferrocene and cobaltocene molecular levels closely follow the chemical potentials of the right and left leads, respectively. The reason for this becomes clear by looking at the potential profile in Figure 3a: the voltage drops mainly over the spacer, with negligible drop in the vicinity of ferrocene and cobaltocene sites.

At intermediate bias, 0.8 to 1.2 V, resonant tunneling occurs as the HOMOs of ferrocene and cobaltocene cross. A high-transmission spot appears in Figure 2c right at the crossing area, which causes the sharp increase in current shown in Figure 1b.

At bias just below 1.2 V, a discontinuity takes place. This sudden drop in current results from the fact that the HOMO of ferrocene and the HOMO of cobaltocene become misaligned.

A backward voltage sweep reveals bistability from 1.2 to 0.5 V. DFT is being used for a nonequilibrium problem here, so the variational principle does not apply. The self-consistent procedure seeks convergence of an open boundary system within the nonequilibrium Green function description[8] — a match between the densities resulting from DFT and the lesser Green function. It is thus possible to get two solutions depending on the initial input, in contrast to the unique ground-state solution. Figure 4 shows the PDOS evolution in this case: a dramatic change of the orbital evolution compared with Figure 2b, especially the spin-down component, is seen for the two states of the cobaltocene moiety (more clearly shown in Figure 2a). As the voltage is scanned forward, its energy level becomes lower during the crossing process, approaching the left chemical potential (white solid line in Figure 2b); in contrast, under reverse scanning, it remains in line with the left chemical potential until 0.5 V. A softer NDR appears as the voltage is swept backward because it is purely due to level crossing of broadened molecular levels, as shown in Figure 4b, while in the forward sweep case the sharp current drop is due to charge redistribution. To explore the origin of the bistability, we plot the charge difference between the backward and forward sweeps at 1.1 V in Figure 5. Notice a clear charge redistribution: the

Figure 5. Charge difference of spin-up (a) and spin-down electrons (b) at 1.1 V between backward and forward scanning. White denotes electron loss, and red denotes electron gain.

cobaltocene moiety loses 0.18 e of spin-up and gains 0.12 e of spin-down electron, while the ferrocene moiety undergoes a 0.24 e gain of spin-up and a 0.27 e loss of spin-down electron — a net loss of 0.09 e when sweeping backward. We attribute this charge redistribution to a degenerate perturbation between the two crossing levels.

Thus, we have shown that molecular-level crossing in an organometallic MDD system leads to NDR and hysteresis. It is important to point out that one could have NDR in the absence of bistability in such diblock structured molecules; upon reverse sweep the two crossing levels would simply pass each other, as for a forward sweep. In this case, localized molecular orbitals become more important since they completely determine the span of the NDR peak. We have considered a number of possible modifications to our basic molecule of Figure 1a. First, we increased the insulating spacer by exchanging the C_2H_4 group for C_4H_8, resulting in similar NDR and hysteretic behaviors. Second, we considered a symmetric molecule containing two ferrocenes. It has a much wider HOMO−LUMO gap of ∼1.5 eV. The high voltage needed to overcome this gap prevents a level crossing because of a substantial voltage drop at the contacts, similar to that in Figure 3b; therefore, this molecule does not show NDR. These examples make clear the importance of having molecular levels which are close to the lead chemical potential in energy.

Acknowledgment. We thank the National Science Foundation for support of this research (DMR-0506953).

References

(1) (a) Joachim, C.; Gimzewski, J. K.; Aviram, A. *Nature* **2000**, *408*, 541. (b) Nitzan, A.; Ratner, M. A. *Science* **2003**, *300*, 1384.
(2) Kornilovitch, P.; Bratkovsky, A.; Williams, S. *Ann. N. Y. Acad. Sci.* **2003**, *1006*, 198.
(3) (a) Chen, J.; Reed, M. A.; Rawlett, A. M.; Tour, J. M. *Science* **1999**, *286*, 1550. (b) Fan, F.-R. F.; Yang, J.; Cai, L.; Price, J. D. W.; Dirk, S. M.; Kosynkin, D. V.; Yao, Y.; Rawlett, A. M.; Tour, J. M.; Bard, A. J. *J. Am. Chem. Soc.* **2002**, *124*, 5550. (c) Guisinger, N. P.; Greene, M. E.; Basu, R.; Baluch, A. S.; Hersam, M. C. *Nano Lett.* **2004**, *4*, 55. (d) Khondaker, S. I.; Yao, Z.; Cheng, L.; Herderson, J. C.; Yao, Y.; Tour, J. M. *Appl. Phys. Lett.* **2004**, *85*, 645.
(4) (a) Blum, A. S.; Kushmerick, J. G.; Long, D. P.; Patterson, C. H.; Yang, J. C.; Henderson, J. C.; Yao, Y.; Tour, J. M.; Shashidhar, R.; Ratna, B. R. *Nature Mater.* **2005**, *4*, 167. (b) Ma, L. P.; Liu, J.; Yang, L. *Appl. Phys. Lett.* **2002**, *80*, 2997.
(5) van der Wiel, W. G.; De Franceschi, S.; Elzerman, J. M.; Fujisawa, T.; Tarucha, S.; Kouwenhoven, L. P. *Rev. Mod. Phys.* **2003**, *75*, 1.
(6) Long, N. J. *Metallocenes: An Introduction to Sandwich Complexes*; Blackwell Science: Oxford, 1998.
(7) (a) Park, J.; Pasupathy, A. N.; Goldsmith, J. L.; Chang, C.; Yaish, Y.; Petta, J. R.; Rinkoski, M.; Sethna, J. P.; Abruna, H. D.; McEuen, P. L.; Ralph, D. C. *Nature* **2002**, *417*, 722−725. (b) Liang, W.; Shores, M. P.; Bockrath, M.; Long, J. R.; Park, H. *Nature* **2002**, *417*, 725−729. (c) Getty, S. A.; Engtrakul, C.; Wang, L.; Liu, R.; Ke, S.-H.; Baranger, H. U.; Yang, W.; Fuhrer, M. S.; Sita, L. R. *Phys. Rev. B* **2005**, *71*, 241401(R).
(8) Ke, S.-H.; Baranger, H. U.; Yang, W. *Phys. Rev. B* **2004**, *70*, 085410.
(9) (a) Damle, P. S.; Ghosh, A. W.; Datta, S. *Phys. Rev. B* **2001**, *64*, 201403. (b) Xue, Y.; Datta, S.; Ratner, M. A. *Chem. Phys* **2002**, *281*, 151. (c) Brandbyge, M.; Mozos, J. L.; Ordejón, P.; Taylor, J.; Stokbro, K. *Phys. Rev. B* **2002**, *65*, 165401. (d) Taylor, J.; Guo, H.; Wang, J. *Phys. Rev. B* **2003**, *63*, 245407.
(10) Soler, J. M.; Artacho, E.; Gale, J. D.; García, A.; Junquera, J.; Ordejón, P.; Sánchez-Portal, D. *J. Phys.: Condens. Matter* **2002**, *14*, 2745.
(11) Perdew, J. P.; Burke, K.; Ernzerhof, M. *Phys. Rev. Lett.* **1996**, *77*, 3865.

JA057054Z